1-1-2014

Altered cytological parameters in buccal cells from individuals with mild cognitive impairment and Alzheimer's disease

Maxime François
Edith Cowan University, maxime.francois@csiro.au

Wayne Leifert

Jane Hecker

Jeffrey Faunt

Ralph Martins
Edith Cowan University, r.martins@ecu.edu.au

See next page for additional authors

10.1002/cyto.a.22453

Title:

Altered cytological parameters in buccal cells from individuals with mild cognitive impairment and Alzheimer's disease.

Running Title: Buccal cytological parameters in Alzheimer's disease

Authors:

Maxime François1,2,3, Wayne Leifert1,2*, Jane Hecker4, Jeffrey Faunt5, Ralph Martins3, Philip Thomas1,2 and Michael Fenech1,2*

1 CSIRO Animal, Food and Health Sciences, Adelaide, SA, Australia.

2CSIRO Preventative Health Flagship, Adelaide, SA, Australia.

3Edith Cowan University, Centre of Excellence for Alzheimer's Disease Research and Care, Joondalup, WA, Australia.

4Department of Internal Medicine, Royal Adelaide Hospital, Adelaide, SA, Australia

5Department of General Medicine, Royal Adelaide Hospital, Adelaide, SA, Australia

***Corresponding Authors:**

CSIRO Animal, Food and Health Sciences.
Gate 13, Kintore Ave. Adelaide. SA 5000

Wayne Leifert
Phone: 0883038821 / Email: wayne.leifert@csiro.au

Michael Fenech
Phone: 0883038880 / Email: michael.fenech@csiro.au

Abstract

Previous studies have shown that mild cognitive impairment (MCI) may be reflective of the early stages of more pronounced neurodegenerative disorders such as Alzheimer's disease (AD). There is a need for a minimally invasive and inexpensive diagnostic to identify those who exhibit cellular pathology indicative of MCI and AD risk so that they can be prioritised for primary preventative measures. The hypothesis was that a minimally invasive approach using cytological markers in isolated buccal mucosa cells can be used to identify individuals of both MCI and AD. An automated buccal cell assay was developed using laser scanning cytometry (LSC) to measure buccal cell type ratios, nuclear DNA content and shape, and neutral lipid content of buccal cells from clinically diagnosed AD (n=13) and MCI (n=13) patients prior to treatment compared to age- and gender-matched controls (n=26). DNA content was significantly higher in all cell types in both MCI ($P<0.01$) and AD ($P<0.05$) compared with controls mainly due to an increase in >2N nuclei. Abnormal nuclear shape (circularity) was significantly increased in transitional cells in MCI ($P<0.001$) and AD ($P<0.01$) when compared to controls. In contrast, neutral lipid content (as measured by Oil red O "ORO" staining) of buccal cells was significantly lower in the MCI group ($P<0.05$) compared with the control group. The ratio of DNA content/ORO in buccal basal cells for both MCI and AD was significantly higher compared to the control group, with ratios for MCI being approximately 2.8-fold greater ($P<0.01$) and AD approximately 2.3-fold greater ($P<0.05$) than the control group. Furthermore, there was a strong negative correlation between buccal cell DNA content and ORO content in the AD group ($r^2=0.75$, $P<0.0001$) but not in MCI or controls. The changes in the buccal cell cytome observed in this study could prove useful as potential biomarkers in identifying individuals with an increased risk of developing MCI and eventually AD.

Keywords: Cell imaging, biomarkers, oral epithelium, Alzheimer's disease, cognitive impairment, laser scanning cytometry, neutral lipids, hyperdiploidy.

Introduction

Alzheimer's disease (AD) is a neurodegenerative disorder characterised clinically by a gradual and progressive loss of memory, cognitive decline, behavioural changes and is the most common cause of dementia (1,2). In clinical practice, patients with AD are not usually identified until the disease has progressed to an advanced stage of cognitive impairment. Neurodegenerative diseases such as Alzheimer's and Parkinson's disease have a predicted increased incidence of 300% in the next thirty years due to an ever ageing population, especially in developing countries (3). This has become a global concern and threatens to impact heavily both socially and economically (4-6). A minimally invasive approach to identify individuals at increased risk for AD before the disease process becomes irreversible and to enhance the possibility of success of preventative diet and life-style strategies would be highly desirable.

One of the minimally invasive strategies is to use biomarkers in the cells of the buccal mucosa collected by the gentle brushing of the inside of the cheeks. Since the buccal mucosa is of ectodermal origin, defects in these cells may reflect potential changes in the pathology of other tissues of ectodermal origin such as the central nervous system. Biomarkers that may identify individuals earlier in life who are at an increased risk of developing mild cognitive impairment (MCI) and AD would be useful as this would allow timely preventative intervention. In a recent pilot study by our group the validation of the full spectrum of biomarkers scoreable in the buccal micronucleus cytome assay was determined using a cytological classification of buccal mucosa cells (7-9). These studies showed that individuals who had just been clinically diagnosed with AD and prior to any medication have a significantly different buccal cytome profile compared to unaffected age- and gender-matched controls. In particular, there was a significant reduction in both basal and karyorrhectic buccal cell frequency which are associated with regenerative potential and cell death, respectively. The odds ratio for diagnosing individuals with AD having a combined basal and karyorrhectic frequency of <41/1000 cells is 140 with a specificity of 97% and a sensitivity of 82% (8),

representing a potential biomarker for AD risk. These differences relative to controls were also evident in Down's syndrome, which is a syndrome of accelerated aging and high propensity for development of AD (10). Both conditions were also associated with elevated DNA damage as measured by an increase in the buccal cell micronucleus frequency, which is a biomarker of whole chromosome loss and/or breakage, and increases in chromosome 17 and chromosome 21 aneuploidy (11). Furthermore, abnormal DNA content (e.g. hyperdiploidy in nuclei) is a marker of DNA damage resulting from chromosome mis-segregation and has been demonstrated to occur in the aging human brain (12) and in the brain of AD patients (13), but to our knowledge has not been previously determined in a quantitative and automated manner in human buccal mucosa cells.

There have been several studies demonstrating that a variety of lipid classes are substantially altered at a very early stage during AD pathogenesis (14,15). Furthermore, relative to controls, altered levels of plasma apoE in AD have been observed (16,17). Previous studies in both animal and cellular AD models indicated that intracellular cholesterol distribution can regulate β-amyloid (considered the main biomarker of AD) generation in the brain (18). A recent study showed that skin fibroblasts from patients with a diagnosis of probable sporadic AD display an imbalance between free cholesterol and cholesterol ester pools (19). Furthermore, Oil Red-O staining (indicative of accumulation of neutral lipids) was used to demonstrate higher levels of neutral lipids in isolated peripheral blood mononuclear cells of probable AD patients (20). Since there is a lack of data available on accumulation of neutral lipids within buccal cells *in vivo*, this parameter was also investigated in healthy controls and individuals diagnosed with MCI and AD.

The aim of this study was to develop and validate the use of an automated high-content Laser scanning cytometry (LSC) protocol (21) to assess whether buccal cell cytoplasm, nuclear and lipid parameters could be used for identifying those at increased risk of developing AD. Since LSC has previously been used successfully to analyse intracellular markers of single cells within subpopulation of neurons (22,23), an automated LSC cytome approach was developed in our study

to analyse single cells from various cell types in the buccal mucosa. Their DNA content and neutral lipid content and their ratios were quantified to identify which parameters, if any, were most strongly associated with those subjects who were diagnosed with MCI or classified as AD. The results of this study show that LSC analysis of buccal cells can yield important diagnostics for identifying those individuals with MCI and AD.

Materials and Methods

Human ethics

Approval for this study was obtained from CSIRO, University of Adelaide and Ramsay Healthcare Ethics Committees. Mild cognitively impaired and Alzheimer's patients were recruited at College Grove Private Hospital, Walkerville, Adelaide, South Australia, following their initial diagnosis and prior to commencement of therapy. Diagnosis of both MCI and AD was made by clinicians (Dr. Jane Hecker and Dr. Jeffrey Faunt) according to the criteria outlined by the National Institute of Neurological and Communicative Disorders and Stroke-Alzheimer's Disease and related Disorders Association (NINCDS–AD&DA) (24), which are the well recognized standards used in all clinical trials. Inclusion criteria were as follows: (1) Mild cognitively impaired (MCI) group (n=13): male (n=2) or female (n=11), clinically diagnosed with MCI. (2) AD group (n=13): male (n=2) or female (n=11), clinically diagnosed with AD. (3) Control Group (n=26): male (n=4) or female (n=22) healthy controls not clinically diagnosed with MCI or AD. Exclusion criteria for all groups were as follows; patients who were undergoing chemotherapy/radiotherapy treatment for cancer, patients supplementing with micronutrients associated with genome maintenance (e.g. folate, vitamin B12) above recommended dietary intakes.

Chemicals and Reagents

NaCl, Tris(hydroxymethyl)aminomethanehydrochloride (Tris), ethylenediaminetetraacetic acid (EDTA), sodium citrate, 4',6-diamidino-2-phenylindole (DAPI), formaldehyde, glycerol, 1-[2,5-Dimethyl-4-(2,5-dimethylphenylazo)phenylazo]-2-naphthol (Oil Red O), triethyl-phosphate and fast green were from Sigma-Aldrich (Castle Hill, NSW, Australia). Phosphate buffered saline (PBS) was from Invitrogen (Mulgrave, Victoria, Australia). All chemicals were of the highest quality grade.

Buccal cell isolation

Consented participants had a one-off buccal cell sample collected after a brief information session outlining the purpose of the study. Buccal cells were collected from the study participants by a trained nurse as described previously (9) to prevent any potential bias introduced by having multiple samplers. Cell concentration was measured using a hemocytometer and cells transferred by cytocentrifugation to a microscope slide using a Shandon Cytospin 4 (600 rpm) at a concentration of 60,000 cells/mL to obtain a final cell density of approximately 3,000 cells per cytospot in duplicate. Slides were then air-dried for 15 min and subsequently transferred to 0.4% formaldehyde in PBS for 10 min, rinsed for 1 min with ultra pure water generated from a Milli-Q water purification system (Millipore Australia Pty Ltd, NSW, Australia) and air dried for 1 hr, then stored in sealed microscope boxes with desiccant at -20°C until the staining procedure was performed.

Staining procedures

Microscope slides containing buccal cells were defrosted by allowing them to warm to room temperature and then stained in randomized batches of 8 including a positive-stained control slide. Positive control slides were prepared with buccal cells from a single person to ensure that the staining procedure was the same for each batch. Microscope slides were washed 3 times for 30 sec each in 1% triethyl-phosphate in ultra pure water and then incubated with Oil Red O (ORO) staining working solution (3 mg/mL ORO in 36% triethyl-phosphate) for 45 min in the dark, to stain for neutral lipids. Slides were then washed 3 times with 1% triethyl-phosphate to remove excess ORO and nuclei stained with DAPI (0.2 μg/mL) for 5 min. The excess DAPI was removed by rinsing the slides in 300 mM NaCl, 34 mM sodium citrate and then slides were further stained in 0.2% (w/v) fast green for 30 min in the dark, to stain cytoplasm. The excess fast green was removed by rinsing the slides for 1 minute with running tap water. Slides were then mounted with coverslips and PBS:Glycerol (1:1) medium. To avoid drying, the coverslips were sealed around the edge with nail polish and kept in a box in the dark at -20°C for up to three days until analysed by LSC.

Laser scanning cytometry measurement of nuclear DNA content, nuclear circularity, neutral lipids and cell sub-types.

Microscope slides were inserted into a 4 slide carrier and analysed by iCyte® Automated Imaging Cytometer (CompuCyte Corporation, Westwood, MA, USA). Lasers selected for the high-content assays were 405 nm, 488 nm and 633 nm to detect DAPI, ORO and Fast Green, respectively. The blue photomultiplier tube (PMT) was used to collect fluorescence from DAPI while the Long Red PMT was utilised to capture fluorescence from Fast Green. As ORO is a chromatic stain, the 488 photo detector was set to quantify its absorbance.

Buccal cells were not always completely dissociated into single isolated cells, but rather, it was noted they exist as populations of single cells and groups of cells. To identify the individual cell types within the population of buccal cells (the buccal cytome) using LSC it was necessary to apply mechanical dissociation procedures (homogenising, passing the cell suspension through a small orifice e.g. 21-gauge needle and a porous Millipore membrane) to the isolated buccal cell samples. Nevertheless, following this stringent protocol, some cells remained in small clusters of 2-6 cells on the microscope slides. Therefore our initial aim was to analyse all cells on the microscope slides, regardless of whether the cells were isolated single cells or those that were in small groups of 2-6 cells that were not completely dissociated during the mechanical separation procedures. Additionally, using the iCyte software we were able to analyse the isolated single cells in more detail by LSC and classify these cell types (as basal, transitional, differentiated and karyolytic) based on cytoplasm area and several nuclear staining parameters and features such as circularity (a measure of abnormal shape), integral (a measure of DNA content based on integrated optical density of pixels within a defined contoured area) and area. Figure 1 shows the different ways of analysing buccal cells with LSC. Cells belonging to a group of cells could not be contoured separately but their nuclei and oil droplets were successfully contoured and could be analysed to provide cytoplasm, lipid and

nuclear data for all cell types combined. For classification and scoring of separated single cell types using the buccal cytome approach, a further categorisation was performed which then identified cells as having 0 or 1 nuclei. Cells without nuclei were classified as karyolytic, and single cells were segregated from large clumps by excluding all cells with more than one nucleus scored, unfortunately excluding at the same time binucleated buccal cells. Binucleated buccal cells could not be separated from the analysis as it was not possible to properly distinguish them from clumps composed of two buccal cells. However we have also noted previously that true binucleated buccal cells are relatively rare events occurring less than 1% of all scored cells (9). Mononucleated cells which were subsequently scored in the automated buccal cytome assay (i.e. single cells) were further categorised into 3 new regions based on the cytoplasm area as well as the $Nuclear_{Area}/Cytoplasm_{Area}$ ratios. Following this procedure, buccal cells were categorized as basal, transitional or differentiated cells. To verify that this categorization of cells was similar to that used in our previous (non-automated) study (8-10), galleries of cells were viewed to allow the proper categorization based on the cytoplasm area as well as the $Nuclear_{Area}/Cytoplasm_{Area}$ ratios. For each participant 500 cells on average were scored to determine the frequency of each cell type in the buccal cytome depending on the slide preparation.

Prior to each batch scan, the same control slide containing previously stained buccal cells sampled from a single person was scanned to ensure all settings and measurements made by LSC had not drifted from the actual original standard values. There was no detectable drift over the course of the study. The fluorescence (and absorbance where appropriate) of events were recorded as follows: area, count (number of events), circularity, and fluorescence integral or inverted absorbance. DNA content and neutral lipid content was assessed in two ways. Firstly the entire cytospot was considered as a tissue section, and all nuclei were examined to obtain nuclear content data (a minimum of 500 and a maximum of 2000 nuclei were analysed per participant depending on the slide preparation); the relative DNA content of the nuclei was determined by the integral of DAPI

fluorescence values. Neutral lipid content was determined from the ratio of ORO area/Fast Green (cytoplasm) area in 500 single cells per participant. Single cells on the microscope slide (as in Figure 1B, C, D and E) were classified in a similar manner to previously, using the buccal cytome approach (8-10). This allowed us to score the cell population consisting of basal, transitional, and differentiated or karyolytic cell types by adapting an automated scoring system that was developed using the iCyte software (21). Thus, it was then possible to investigate DNA content and neutral lipids in more detail within the defined cell populations.

Statistics

One-way analysis of variance (ANOVA) and linear correlation analyses were carried out to determine the significance of the cellular parameters measured between the control, MCI and AD groups. Pairwise comparison of significance between these groups was determined using Tukey-Kramer test as all pairs of columns of unequal sample sizes were compared. ANOVA and correlation values were calculated using GraphPad Prism 5 (GraphPad Software Inc., San Diego, CA, USA). Significance was accepted at $p<0.05$. Receiver-operating characteristic curves (ROC) were carried out for selected parameters between the control and MCI groups to obtain area under the curve (AUC), confidence interval, P-value, sensitivity and specificity scores. When tested with the Fisher's exact test, no significant differences were observed in the gender-ratio between groups.

Results

The mean ± SEM of the age and the mini–mental state examination (MMSE) scores for each of the groups are as follows: control group (76.1 ± 1.5 / 28.4 ± 0.3), MCI (75.3 ± 1.8 / 26.3 ± 0.5) and AD (77.7 ± 2.8 / 21.2 ± 1.1). No significant differences were observed for the age of participants between groups, however there was a significant decrease in the MMSE score of the AD group compared with the control group ($p<0.05$).

Buccal cytome

Using the protocol as described in the methods section single cells were scored based on several cytoplasmic and nuclear staining parameters. Nuclei and cytoplasm size are indicated as the mean ± SEM. We identified and classified the buccal cytome with the following cell types; basal (Figure 1B), transitional (Figure 1C), differentiated (Figure 1D) and karyolytic cells (Figure 1E). Basal cells are the cells from the basal layer which are smaller in size (1200 μm^2 ± 285) when compared to terminally differentiated buccal cells (3900 μm^2 ± 930) and have a nuclear to cytoplasm ratio (0.064 a.u. ± 0.02) that is larger than in differentiated buccal cells (0.018 a.u. ± 0.007). According to our LSC classification criteria, basal cell frequency was 12.7%, 15% and 15.4% for control, MCI and AD, respectively. Transitional cells were classified as a group of cells that were neither large fully differentiated cells nor small basal cells. Transitional cells showed a larger cytoplasm (2150 μm^2 ± 455) and smaller nuclear to cytoplasm ratio (0.031 a.u. ± 0.001) than basal cells with a frequency of 34.5%, 27.1% and 29.5% for control, MCI and AD, respectively. Differentiated cells were distinguished from basal cells and transitional cells by having the largest cell size (3900 μm^2 ± 930) and smallest nuclear to cytoplasmic ratio (0.018 a.u. ± 0.007); (Figure 3C) with a frequency of 27% for control, 29% for MCI and 30.4% for the AD group. Karyolytic cells were another group of cells scored that were characterised by having nuclei completely depleted of DNA and therefore showed no DAPI staining. These cells likely represent a very late stage in the cell death process. There was no

significant difference in the karyolytic, basal, transitional or differentiated buccal cell frequency between the 3 groups.

DNA content

Nuclear DNA content of all buccal cells on the microscope slides within the cytospots was determined by measuring the DNA integral of all nuclei. Figure 2A shows that there was a significantly higher nuclear DNA content in buccal cells from the MCI group ($p<0.01$) and AD groups ($p<0.05$) compared with the control group when all cells were analysed but there was no significant difference between the MCI and AD groups. Furthermore, when only the single mononucleated cells were analysed, DNA content values were also increased in nuclei for MCI ($p<0.01$) and AD ($p<0.05$) compared to controls, as shown in Figure 2B. Therefore, the values obtained from the single separated cell analyses were comparable to those obtained from all cells including those in small clumps. As a next step in the analysis of individual buccal cells by LSC, we investigated the DNA content of the different cell types that contained nuclei i.e. basal, transitional and differentiated buccal cells. Figure 2C shows the results of nuclear DNA content analyses by LSC in basal cells. Both MCI and AD groups had a significantly higher DNA content in basal buccal cells compared with controls ($p<0.001$ and $p<0.01$, respectively). In transitional cells (Figure 2D) there was a significantly higher nuclear DNA content in the MCI ($p<0.01$) group compared with controls. Similarly, in fully differentiated buccal cells there was a significantly higher DNA content in the MCI ($p<0.01$) group compared with controls (Figure 2E). Overall it was evident that DNA content of buccal cells from the AD and MCI groups was 55% and 72% greater than for controls, respectively.

Neutral lipids

LSC was used to simultaneously determine the content of neutral lipids in buccal cells by staining cells with ORO. ORO is a lysochrome fat-soluble dye which has been used for demonstrating the

presence of neutral lipids such as cholesteryl esters and triglycerides in cells (19,20). Upon staining, the neutral lipids appear as bright red spots in the cytoplasm. When all cells were examined (including groups of cells), there was a significantly lower ($p<0.05$) ORO in the MCI group compared with the controls and there was no significant difference between controls and AD (Figure 3A). Similarly, Figure 3B shows a significant decrease ($p<0.05$) in ORO between MCI and controls when only the single separate buccal cells were analysed. We further investigated ORO content in the specific buccal cell types. Figure 3C demonstrates that ORO staining was significantly lower in the MCI group compared with the control group in the basal cells ($p<0.05$), transitional cells (Figure 3D; $p<0.05$) and karyolytic cells (Figure 3F; $p<0.01$), whilst there was no significant difference in differentiated cells (Figure 3E) between MCI, AD and their relative controls. Additionally, there was no significant difference between either the control and AD groups or the MCI and AD groups for any of the buccal cell types.

DNA/ORO ratio

Since the DNA content was increased in the MCI and AD groups compared with the control group, and ORO content showed a trend to being lower in the AD group and was significantly lower in the MCI group compared with the control group, we investigated whether applying a DNA content/ORO ratio would amplify the differences observed in the buccal cells. Figure 4A shows the DNA/ORO ratios in all buccal cell types examined (single cells and cells in small groups) and interestingly, the DNA/ORO ratio was significantly higher (2.8-fold) in the MCI group compared with control group ($p<0.001$), however DNA/ORO ratio was not significantly higher for the AD group compared with the control group. To further identify the cell types contributing to this difference in DNA/ORO ratios, we analysed the DNA/ORO in the individual separated cells containing nuclei (Figure 4B) and found that there was a significantly higher DNA/ORO ratio in MCI ($p<0.001$) buccal cells compared with control buccal cells. On further analysis of the individual cell types, there was a significantly higher DNA/ORO

ratio in basal cells for MCI ($p<0.01$) and AD ($p<0.05$) compared with control (Figure 4C). Additionally, there was a significantly higher DNA/ORO ratio in transitional cells for MCI ($p<0.01$) compared with control (Figure 4D), as well as a significantly higher DNA/ORO ratio in differentiated cells for MCI ($p<0.01$) and AD ($p<0.05$) compared with control (Figure 4E).

To further investigate the differences observed, we then explored whether there was a correlation between DNA content and ORO content in buccal cells. Interestingly, when all cell types (including groups of cells) were examined, there was a significant negative correlation of DNA content with ORO content in the AD group ($r = -0.86$; $p<0.0001$) and MCI group albeit to a weaker extent ($r = -0.5$, $p=0.0093$). This strong negative correlation was also apparent in individual mononucleated cells (collectively; basal, transitional, differentiated), ($r = -0.86$, $p<0.0001$) as well as basal ($r = -0.65$, $p<0.001$), transitional ($r = -0.77$, $p<0.0001$) and differentiated cells ($r = -0.70$, $p<0.0001$) separately, for AD cases but not for MCI or controls.

Hyperdiploidy

To investigate if the increase of DNA content observed in MCI and AD was due to either a lower proportion of hypodiploid nuclei or a higher proportion of hyperdiploid nuclei compared to controls, ploidy was measured by plotting nuclei on a histogram depending on their DAPI Integral. Peaks of <2N, 2N and >2N nuclei were then defined and the percentage of nuclei in each of these categories was obtained (Figure 5). Representative DNA histograms from each group, control, MCI and AD are shown in Figure 5A, 5B and 5C, respectively. It appeared that a shift occurred in nuclei from the 2N peak towards the >2N peak in MCI and AD when compared to control. Figure 5D summarises the data where percentage of nuclei in the different peaks (<2N, 2N and >2N) for each of the three groups are shown. Buccal cells from MCI as well as AD cases exhibited a decrease in the percentage of 2N nuclei ($p<0.001$ and $p<0.01$, respectively) with a concomitant increase in the percentage of >2N nuclei when compared to buccal cells from controls ($p<0.01$ and $p<0.05$, respectively).

Interestingly, no changes occurred in the <2N nuclei population which indicated that the increase in DNA content observed in MCI and AD was not due to a decrease in hypodiploidy but due to an increase in hyperdiploidy. We also measured irregular nuclear shape (circularity) relative to the normal smooth and circular to oval nuclear perimeter, with a high circularity value indicating a more irregular-shaped structure. The results indicated a significantly increased circularity (and thus a more irregular shape) of nuclei in transitional cells from MCI and AD cases relative to controls ($p<0.001$ and $p<0.01$ respectively, Figure 5E). Interestingly, when investigated in all cells (including groups of cells), circularity was found to be significantly higher in MCI ($p<0.05$) but not in AD when compared to control (data not shown).

ROC curves

For each of the parameters analysed, receiver-operator characteristic (ROC) curves were generated. The area under the curve, confidence interval, P values, specificity and sensitivity scores were calculated. Only ROC curves for biomarkers and their combinations that showed differences between groups were investigated using the results for all cell types combined (Table 1). These results indicate a strong diagnostic value of these biomarkers or their combinations for identifying MCI cases relative to controls with AUC values ranging from 0.76 for nuclear DNA content to 0.84 for the combination “Circularity + ORO”.

Discussion

The objective of the present study was to develop and test an LSC-based method to measure novel additional biomarkers in the buccal micronucleus cytome assay (9) such as simultaneous measurement of nuclear DNA content/aneuploidy and neutral lipid content in buccal cells of MCI and AD individuals relative to controls. This study demonstrated significant changes in buccal cells isolated from MCI and AD subjects including the buccal cell type ratio, increased nuclear DNA content, nuclear circularity and DNA content/neutral lipid ratio in both MCI and AD subjects relative to controls.

An advantage of LSC scoring of buccal cells is that all the microscope slides are scanned with the same LSC settings (21), i.e. the software is set up in such a manner that all slides are examined using identical parameters and the numerical values obtained by the quantitative imaging allows for the separation of cell types, thus removing the potential for subjectivity existing from one individual scorer to another. Our LSC results did not support previous observations of substantial differences in frequency of the cell types between the control and Alzheimer's group when visual analysis was used (8,25), which may be due to the exclusion of cells in clumps in the LSC method and the different staining methods used

To define the cell types present we aimed to classify the cells depending on their developmental stage based upon some of the visual scoring criteria developed by our group and the HUMNxL project (8). Previously, these criteria when used with a visual scoring suggested that the cell composition of the buccal mucosa was significantly altered in Alzheimer's patients i.e. significant reduction in basal cells, karyorrhectic and condensed chromatin cells (the latter two being biomarkers of cell death) (8). These changes were possibly explained by a decrease in the regenerative potential of the buccal mucosa in AD. The frequency of different cell types obtained in our current study using LSC was somewhat different than the previous visual scoring method which may partly be explained by the different staining procedures used in these studies, and because

karyorrhectic and condensed chromatin cells could not be reliably identified in the LSC method. It was assumed that these would appear as cells with nuclei having a <2N DNA content because karyorrhectic and condensed chromatin cells are thought to be apoptotic leading to nuclear fragmentation. However, there was no evidence that the frequency of <2N nuclei was reduced in MCI or AD.

In this study aneuploidy was measured by quantitating the fluorescent integral of the DAPI signal, providing data on nuclear DNA content as shown previously with Feulgen staining (26). Results showed a significantly higher DNA content in buccal cells from the MCI group ($p<0.01$) and AD group ($p<0.05$) compared with the control group. The ploidy distribution of nuclei showed that MCI and AD cases presented a decrease in the frequency of 2N nuclei which was accompanied by an increase in hyperdiploid nuclei as well as nuclear circularity. Therefore, the higher DNA content observed in MCI and AD cases might be partly explained by the accumulation of buccal cells in the S and G2 phase of the cell cycle. The observed hyperdiploidy may be due to cell cycle checkpoint arrest due to mitotic defect leading to mitotic slippage which can lead to generation of 4N cells (27). Another possibility is malsegregation of chromosomes leading to trisomic and monosomic cells assuming that the former are more likely to survive. An increase in trisomy 21 and trisomy 17 has been reported in buccal cells in AD cases when compared to their respective controls (11). Furthermore micronuclei are a biomarker of chromosome malsegregation and tend to be elevated in lymphocytes, fibroblasts and buccal cells of AD cases (8,28,29). Other DNA damage markers such as γH2AX (DNA double strand breaks) and 8HOdG (oxidative DNA damage) were also found to be linked with AD (30-32) and previously detected in human buccal cells (33,34). Therefore, the genomic instability events observed previously may partly explain the results of increased DNA content observed in this study when measured quantitatively by LSC.

Changes in lipid composition in the brain have been reported in AD, for example both membrane cholesterol and phospholipids were found to be significantly reduced in the cortex of AD

mice (35), and the lipid composition of different regions in the human brain have been shown to change with ageing as well as in AD (36,37). Our study demonstrates for the first time that ORO content decreases in the oral mucosa of MCI in all cell types examined ($p<0.05$) when compared to controls. The ORO content also tended to decrease in AD but this did not reach statistical significance. Thus it is possible that changes in neutral lipid accumulation in buccal cells precedes AD and is elevated at an early stage of AD pathogenesis. Furthermore, it was noted that the DNA content/ORO ratio was significantly elevated compared with controls in both the MCI and AD group in all cell types scored. Additionally a strong negative correlation was observed between DNA content and ORO in the AD group in all cell types but this type of correlation was not observed in controls or to a lesser extent in MCI suggesting a link between hyperdiploidy and lipid content in cells as progression from MCI to AD occurs. However we have no obvious explanation for this finding unless cell cycle arrest and mitotic slippage is caused by lack of lipid-derived energy required for completion of the mitotic process. Alternatively, inadequate stores of lipids may reduce the capacity to synthesise sufficient cytoplasmic membrane requirements for mitosis completion leading to cytokinetic arrest and aneuploidy (38). Lipid metabolism has also been studied in fibroblasts from AD patients whereby the cholesterol esterification rate was reported to increase after 48 hours of cellular tissue culture ($p<0.05$) (19). This level of cholesteryl ester synthesis was linked to an expanded cytoplasmic pool of neutral lipid measured using the ORO staining procedure. In a second study, Pani et al (20) also investigated the DNA synthesis of lymphocytes after growth-stimulation with phytohemagglutinin and found that neutral lipid content increased in parallel with the rate of cell growth *in vitro*, supporting the possibility that the optimal nutrition in culture medium restored the capacity of cells to maintain cholesteryl ester synthesis. We previously hypothesised that the regenerative potential of the buccal mucosa was reduced with development of AD (8,10), and therefore it is possible that the rate of regeneration and proliferation of buccal cells influences the

cytoplasmic accumulation of neutral lipids *in vivo*; this may partly explain why a decrease of neutral lipid content in buccal cells occurs in the early stage of AD.

To-date there has been no simple, inexpensive and minimally invasive procedure available to confirm the early diagnosis of AD. Therefore, if screening of populations of individuals is to be performed, more suitable, easily accessible tissues would need to be used, also using diagnostic tests at much lower costs compared to brain imaging and cerebrospinal fluid diagnostics of amyloid β and Tau (39-41). This need for minimally invasive tests could be achieved by targeting surrogate tissues, since it is now well recognised that AD is not a disorder restricted to pathology and biomarkers within the brain only. Combining neutral lipid accumulation, DNA content with other potential more specific protein markers may substantially increase the likelihood of better predictive markers for AD. Such a combined protocol would provide a high-content, automated assay capable of measuring multiple parameters in human buccal cells simultaneously.

Acknowledgments

The authors thank Maryam Hor for the processing of buccal cells. Financial support from the CSIRO's Preventative Health Flagship is gratefully acknowledged. This project was part funded by a grant from The JO & JR Wicking Trust, which is managed by ANZ Trustees (Australia). The authors declare they have no Conflict of Interest.

Table and Figure Legends

Table 1. ROC curves for individual and combination of biomarkers.

ROC curve results obtained for LSC biomarkers and their combinations for data in all cell types comparing controls and MCI. Abbreviations; AUC, area under the curve; ORO, Oil Red O; %>2N, % of >2N nuclei; **, $p<0.01$; ***, $p<0.001$.

Figure 1. Buccal cell types analysed by LSC.

(A) Schematic showing an example of the different cell types present in a buccal sample and the various parameters that are measured by laser scanning cytometry. In the schematic (upper left panel of (A)), the various types of individual cells that are classified by LSC are shown (basal, differentiated, transitional and karyolytic). Additionally, a group of 6 cells is shown in the centre since it was not possible to allocate a cellular classification to cells when they appeared in groups. (Ai) When the integral fluorescence from all nuclei (blue circles) was examined, both DNA content and nuclear circularity was measured. Since cells that are grouped cannot be classified by LSC as basal, differentiated, transitional or karyolytic, a ratio of the total lipid area (red circles) and the total cytoplasm area (green) was applied to all cells on the microscope slides to obtain the $lipid_{Area}$/$cytoplasm_{Area}$ ratio. (Aii) When isolated single cells (i.e. cells that do not exist in a group of cells) were classified, the following cell types were scored; basal, transitional, differentiated and karyolytic. Additionally, within each of those classified cells types the following parameters were measured; lipid content, DNA content and nuclear circularity. (B-E) LSC images of representative different buccal cell types. (B) basal, (C) transitional, (D) differentiated and (E) karyolytic cells are shown. Note the green contour line indicating the cytoplasmic periphery of the cells, the blue contour lines around nuclei and the magenta contour lines around Oil Red O spots in the cytoplasm.

Figure 2. DNA content of nuclei measured by LSC in buccal cells from controls (n=26), MCI (n=13) and AD (n=13). DNA content of nuclei from (A) all buccal cell types including cells in groups, (B) single mononucleated cells (C) basal cells, (D) transitional cells and (E) differentiated cells. Abbreviations; AD, Alzheimer's disease; a.u. arbitrary units; MCI, Mild cognitively impaired; *p<0.05, **p<0.01, ***p<0.001.

Figure 3. Oil Red O Content in buccal cells measured by LSC. Cell types were compared in buccal cells from controls (n=26), MCI (n=13) and AD (n=13). Quantification of the accumulated ORO was calculated as described in methods. ORO staining (% of cytoplasm area) (A) for all cells, (B) for all single mononucleated cells, (C) basal cells, (D) transitional cells, (E) differentiated cells and (F) karyolytic cells. Abbreviations; AD, Alzheimer's disease; MCI, Mild cognitively impaired; ORO, Oil red O; *p<0.05.

Figure 4. DNA content/ORO ratio for buccal cells from controls (n=26), MCI (n=13) and AD (n=13). The DNA content/ORO ratios are shown (A) for all buccal cell types including those cells in groups, (B) all single mononucleated cells, (C) basal cells, (D) transitional cells and (E) differentiated cells. Abbreviations; AD, Alzheimer's disease; a.u., arbitrary units; MCI, mild cognitively impaired; *p<0.05, **p<0.01, ***p<0.001.

Figure 5. Ploidy measurement for nuclei in buccal cells by LSC. Comparison of DNA ploidy for Controls (n=26), MCI (n=13) and AD (n=13). Representative DNA histograms are shown for (A) controls, (B) MCI and (C) AD. DNA content data for all study participants are summarised as shown in (D), with the percentage of nuclei represented as <2N, 2N or >2N as described in methods. (E) The circularity parameter of LSC was applied demonstrating an increase in circularity (irregular shape) of nuclei in transitional cells observed in MCI and AD. Abbreviations; AD, Alzheimer's disease; a.u., arbitrary units; MCI, mild cognitive impaired; *p<0.05, **, p<0.01; ***, p<0.001.

References

1. Burns A, Byrne EJ, Maurer K. Alzheimer's disease. Lancet 2002;360:163-165.

2. Alzheimer's Association, Thies W, Bleiler L. 2011 Alzheimer's disease facts and figures. Alzheimers Dement 2011;7:208-244.

3. Kalaria RN, Maestre GE, Arizaga R, Friedland RP, Galasko D, Hall K, Luchsinger JA, Ogunniyi A, Perry EK, Potocnik F, Prince M, Stewart R, Wimo A, Zhang ZX, Antuono P, World Federation of Neurology Dementia Research Group. Alzheimer's disease and vascular dementia in developing countries: prevalence, management, and risk factors. Lancet Neurol 2008;7:812-826.

4. Sloane PD, Zimmerman S, Suchindran C, Reed P, Wang L, Boustani M, Sudha S. The public health impact of Alzheimer's disease, 2000-2050: potential implication of treatment advances. Annu Rev Public Health 2002;23:213-231.

5. Smith AD. The worldwide challenge of the dementias: a role for B vitamins and homocysteine? Food Nutr Bull 2008;29:S143-72.

6. Ferri CP, Prince M, Brayne C, Brodaty H, Fratiglioni L, Ganguli M, Hall K, Hasegawa K, Hendrie H, Huang Y, Jorm A, Mathers C, Menezes PR, Rimmer E, Scazufca M, Alzheimer's Disease International. Global prevalence of dementia: a Delphi consensus study. Lancet 2005;366:2112-2117.

7. Thomas P, O'Callaghan NJ, Fenech M. Telomere length in white blood cells, buccal cells and brain tissue and its variation with ageing and Alzheimer's disease. Mech Ageing Dev 2008;129:183-190.

8. Thomas P, Hecker J, Faunt J, Fenech M. Buccal micronucleus cytome biomarkers may be associated with Alzheimer's disease. Mutagenesis 2007;22:371-379.

9. Thomas P, Holland N, Bolognesi C, Kirsch-Volders M, Bonassi S, Zeiger E, Knasmueller S, Fenech M. Buccal micronucleus cytome assay. Nat Protoc 2009;4:825-837.

10. Thomas P, Harvey S, Gruner T, Fenech M. The buccal cytome and micronucleus frequency is substantially altered in Down's syndrome and normal ageing compared to young healthy controls. Mutat Res 2008;638:37-47.

11. Thomas P, Fenech M. Chromosome 17 and 21 aneuploidy in buccal cells is increased with ageing and in Alzheimer's disease. Mutagenesis 2008;23:57-65.

12. Fischer HG, Morawski M, Bruckner MK, Mittag A, Tarnok A, Arendt T. Changes in neuronal DNA content variation in the human brain during aging. Aging Cell 2012;11:628-633.

13. Mosch B, Morawski M, Mittag A, Lenz D, Tarnok A, Arendt T. Aneuploidy and DNA replication in the normal human brain and Alzheimer's disease. J Neurosci 2007;27:6859-6867.

14. Han X. Lipid alterations in the earliest clinically recognizable stage of Alzheimer's disease: implication of the role of lipids in the pathogenesis of Alzheimer's disease. Curr Alzheimer Res 2005;2:65-77.

15. Han X, Holtzman DM, McKeel DW,Jr. Plasmalogen deficiency in early Alzheimer's disease subjects and in animal models: molecular characterization using electrospray ionization mass spectrometry. J Neurochem 2001;77:1168-1180.

16. Gupta VB, Laws SM, Villemagne VL, Ames D, Bush AI, Ellis KA, Lui JK, Masters C, Rowe CC, Szoeke C, Taddei K, Martins RN, AIBL Research Group. Plasma apolipoprotein E and Alzheimer disease risk: the AIBL study of aging. Neurology 2011;76:1091-1098.

17. Taddei K, Clarnette R, Gandy SE, Martins RN. Increased plasma apolipoprotein E (apoE) levels in Alzheimer's disease. Neurosci Lett 1997;223:29-32.

18. Puglielli L, Tanzi RE, Kovacs DM. Alzheimer's disease: the cholesterol connection. Nat Neurosci 2003;6:345-351.

19. Pani A, Dessi S, Diaz G, La Colla P, Abete C, Mulas C, Angius F, Cannas MD, Orru CD, Cocco PL, Mandas A, Putzu P, Laurenzana A, Cellai C, Costanza AM, Bavazzano A, Mocali A, Paoletti F. Altered cholesterol ester cycle in skin fibroblasts from patients with Alzheimer's disease. J Alzheimers Dis 2009;18:829-841.

20. Pani A, Mandas A, Diaz G, Abete C, Cocco PL, Angius F, Brundu A, Mucaka N, Pais ME, Saba A, Barberini L, Zaru C, Palmas M, Putzu PF, Mocali A, Paoletti F, La Colla P, Dessi S. Accumulation of neutral lipids in peripheral blood mononuclear cells as a distinctive trait of Alzheimer patients and asymptomatic subjects at risk of disease. BMC Med 2009;7:66.

21. Leifert WR, Francois M, Thomas P, Luther E, Holden E, Fenech M. Automation of the buccal micronucleus cytome assay using laser scanning cytometry. Methods Cell Biol 2011;102:321-339.

22. Reinert A, Mittag A, Reinert T, Tarnok A, Arendt T, Morawski M. On the quantification of intracellular proteins in multifluorescence-labeled rat brain slices using slide-based cytometry. Cytometry A 2011;79:485-491.

23. Mosch B, Mittag A, Lenz D, Arendt T, Tarnok A. Laser scanning cytometry in human brain slices. Cytometry A 2006;69:135-138.

24. McKhann G, Drachman D, Folstein M, Katzman R, Price D, Stadlan EM. Clinical diagnosis of Alzheimer's disease: report of the NINCDS-ADRDA Work Group under the auspices of Department of Health and Human Services Task Force on Alzheimer's Disease. Neurology 1984;34:939-944.

25. de Oliveira RM, Lia EN, Guimaraes RM, Bocca AL, Cavalcante Neto FF, da Silva TA. Cytologic and cytometric analysis of oral mucosa in Alzheimer's disease. Anal Quant Cytol Histol 2008;30:113-118.

26. Pozarowski P, Huang X, Gong RW, Priebe W, Darzynkiewicz Z. Simple, semiautomatic assay of cytostatic and cytotoxic effects of antitumor drugs by laser scanning cytometry: effects of the bis-intercalator WP631 on growth and cell cycle of T-24 cells. Cytometry A 2004;57:113-119.

27. Kirsch-Volders M, Fenech M. Inclusion of micronuclei in non-divided mononuclear lymphocytes and necrosis/apoptosis may provide a more comprehensive cytokinesis block micronucleus assay for biomonitoring purposes. Mutagenesis 2001;16:51-58.

28. Migliore L, Testa A, Scarpato R, Pavese N, Petrozzi L, Bonuccelli U. Spontaneous and induced aneuploidy in peripheral blood lymphocytes of patients with Alzheimer's disease. Hum Genet 1997;101:299-305.

29. Trippi F, Botto N, Scarpato R, Petrozzi L, Bonuccelli U, Latorraca S, Sorbi S, Migliore L. Spontaneous and induced chromosome damage in somatic cells of sporadic and familial Alzheimer's disease patients. Mutagenesis 2001;16:323-327.

30. Myung NH, Zhu X, Kruman II, Castellani RJ, Petersen RB, Siedlak SL, Perry G, Smith MA, Lee HG. Evidence of DNA damage in Alzheimer disease: phosphorylation of histone H2AX in astrocytes. Age (Dordr) 2008;30:209-215.

31. Migliore L, Fontana I, Trippi F, Colognato R, Coppede F, Tognoni G, Nucciarone B, Siciliano G. Oxidative DNA damage in peripheral leukocytes of mild cognitive impairment and AD patients. Neurobiol Aging 2005;26:567-573.

32. Perry G, Castellani RJ, Smith MA, Harris PL, Kubat Z, Ghanbari K, Jones PK, Cordone G, Tabaton M, Wolozin B, Ghanbari H. Oxidative damage in the olfactory system in Alzheimer's disease. Acta Neuropathol 2003;106:552-556.

33. Gonzalez JE, Roch-Lefevre SH, Mandina T, Garcia O, Roy L. Induction of gamma-H2AX foci in human exfoliated buccal cells after in vitro exposure to ionising radiation. Int J Radiat Biol 2010;86:752-759.

34. Borthakur G, Butryee C, Stacewicz-Sapuntzakis M, Bowen PE. Exfoliated buccal mucosa cells as a source of DNA to study oxidative stress. Cancer Epidemiol Biomarkers Prev 2008;17:212-219.

35. Yao JK, Wengenack TM, Curran GL, Poduslo JF. Reduced membrane lipids in the cortex of Alzheimer's disease transgenic mice. Neurochem Res 2009;34:102-108.

36. Soderberg M, Edlund C, Alafuzoff I, Kristensson K, Dallner G. Lipid composition in different regions of the brain in Alzheimer's disease/senile dementia of Alzheimer's type. J Neurochem 1992;59:1646-1653.

37. Soderberg M, Edlund C, Kristensson K, Dallner G. Lipid compositions of different regions of the human brain during aging. J Neurochem 1990;54:415-423.

38. Natter K, Kohlwein SD. Yeast and cancer cells - common principles in lipid metabolism. Biochim Biophys Acta 2013;1831:314-326.

39. Thambisetty M, Lovestone S. Blood-based biomarkers of Alzheimer's disease: challenging but feasible. Biomark Med 2010;4:65-79.

40. Hampel H, Prvulovic D. Are biomarkers harmful to recruitment and retention in Alzheimer's disease clinical trials? An international perspective. J Nutr Health Aging 2012;16:346-348.

41. Blennow K, Zetterberg H. Cerebrospinal fluid biomarkers for Alzheimer's disease. J Alzheimers Dis 2009;18:413-417.

Figure 1.

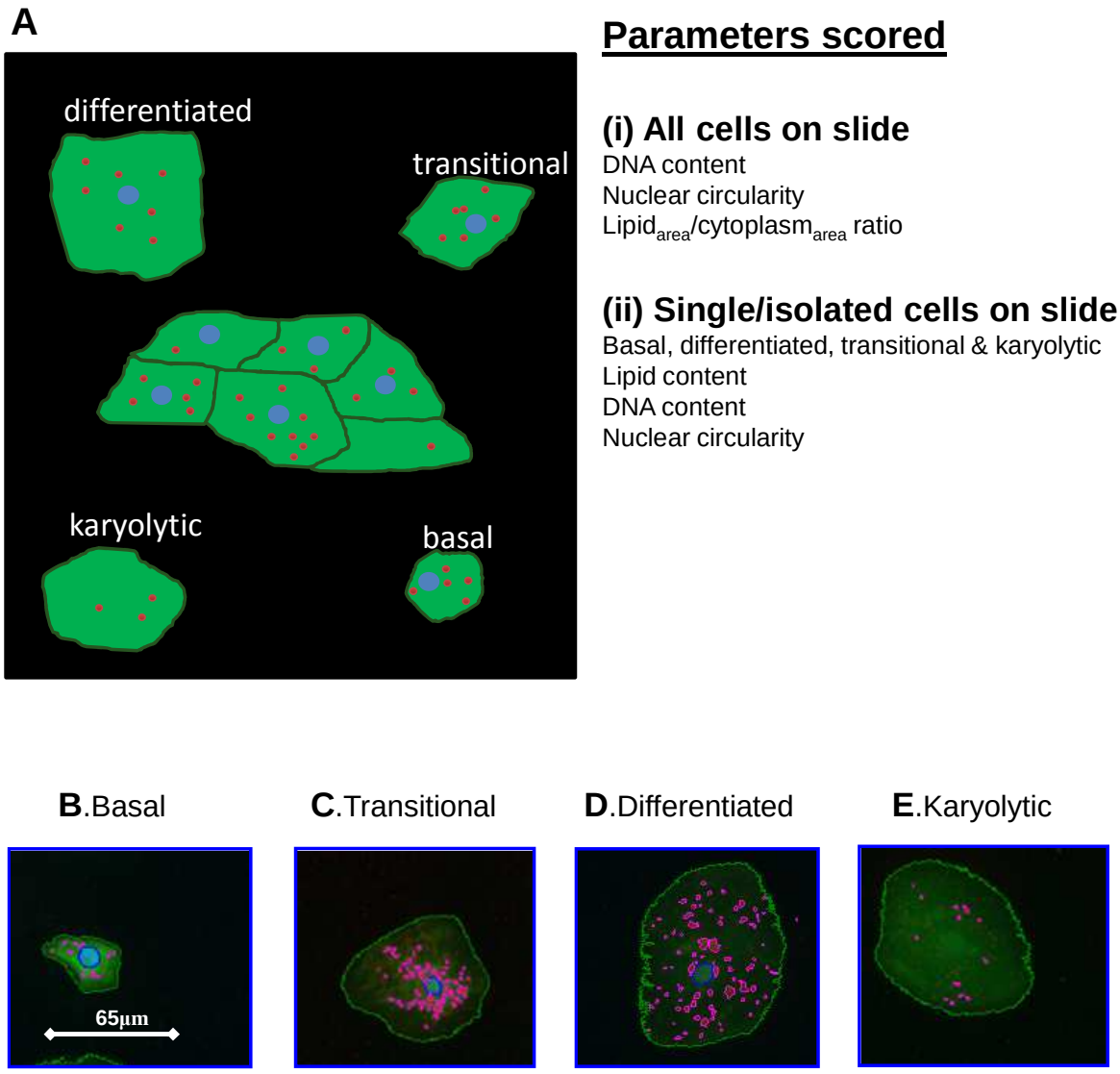
A
differentiated
transitional
karyolytic
basal
Parameters scored
(i) All cells on slide
DNA content
Nuclear circularity
Lipid$_{area}$/cytoplasm$_{area}$ ratio
(ii) Single/isolated cells on slide
Basal, differentiated, transitional & karyolytic
Lipid content
DNA content
Nuclear circularity
B.Basal
C.Transitional
D.Differentiated
E.Karyolytic
65µm

Figure 2.

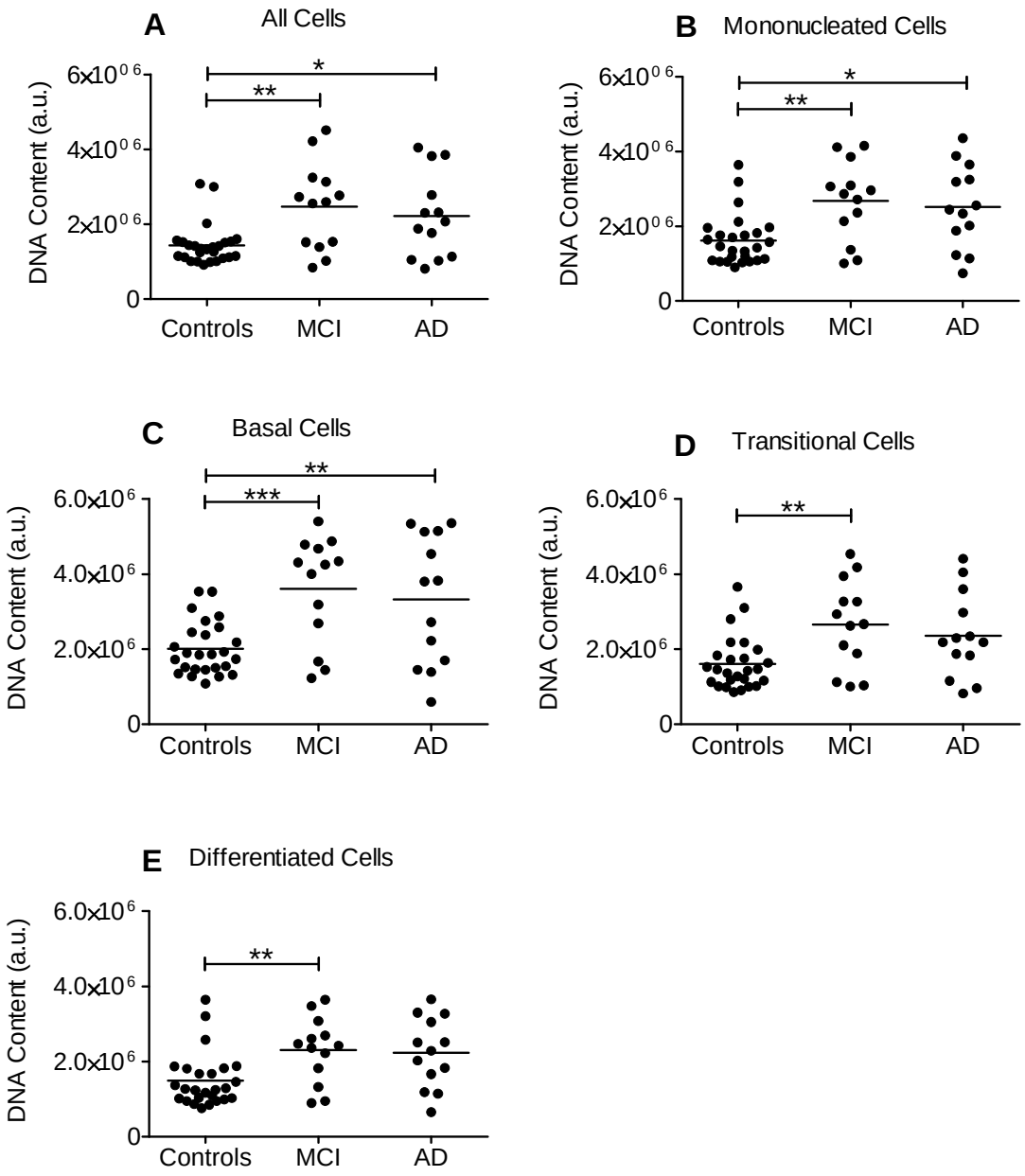
A
All Cells
DNA Content (a.u.)
6x10^0 6
4x10^0 6
2x10^0 6
0
Controls
MCI
AD
*
**
B
Mononucleated Cells
DNA Content (a.u.)
6x10^0 6
4x10^0 6
2x10^0 6
0
Controls
MCI
AD
*
**
C
Basal Cells
DNA Content (a.u.)
6.0x10^6
4.0x10^6
2.0x10^6
0
Controls
MCI
AD
**
***
D
Transitional Cells
DNA Content (a.u.)
6.0x10^6
4.0x10^6
2.0x10^6
0
Controls
MCI
AD
**
E
Differentiated Cells
DNA Content (a.u.)
6.0x10^6
4.0x10^6
2.0x10^6
0
Controls
MCI
AD
**

Figure 3.

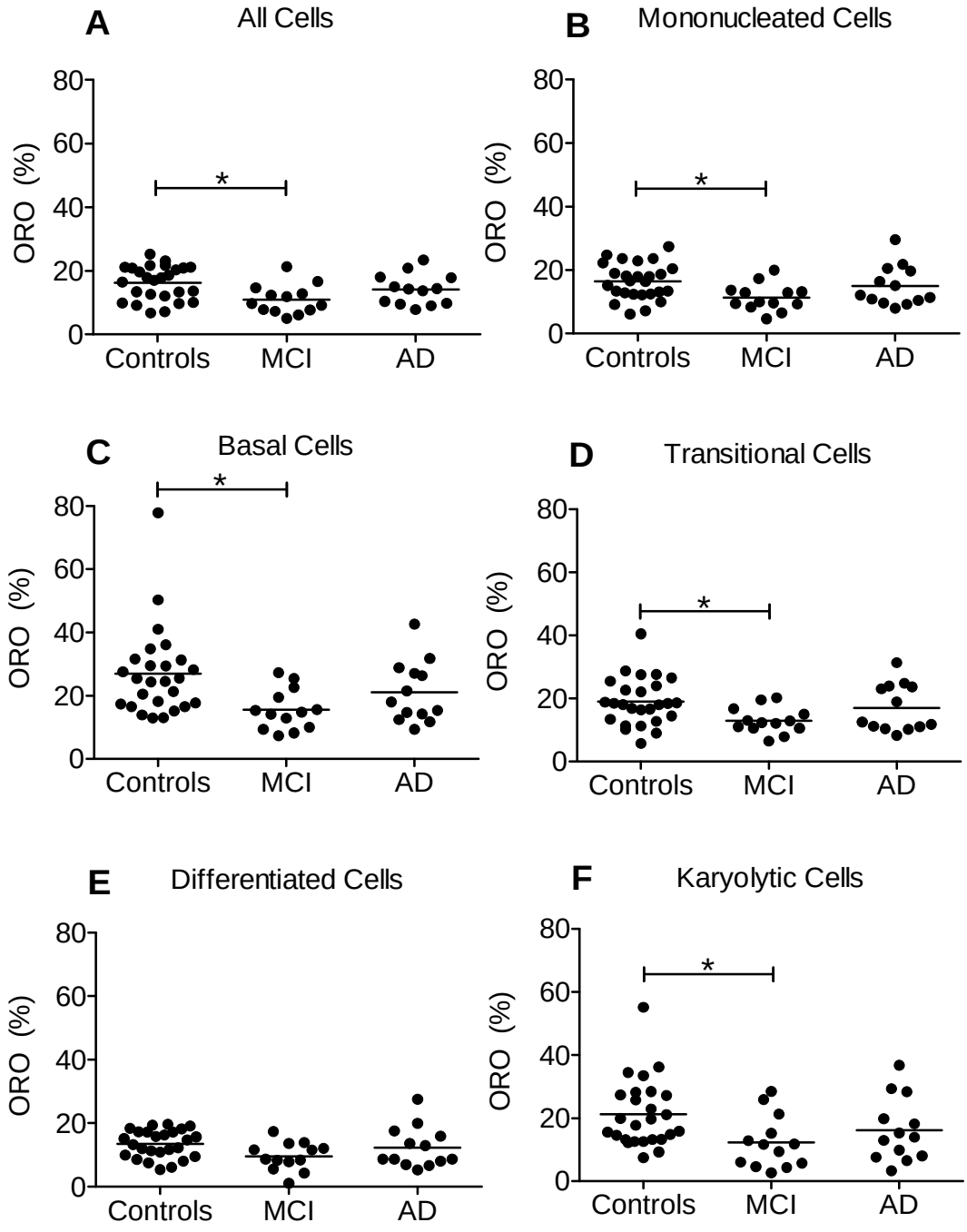
A
All Cells
B
Mononucleated Cells
C
Basal Cells
D
Transitional Cells
E
Differentiated Cells
F
Karyolytic Cells
ORO (%)
0
20
40
60
80
*
Controls
MCI
AD

Figure 4.

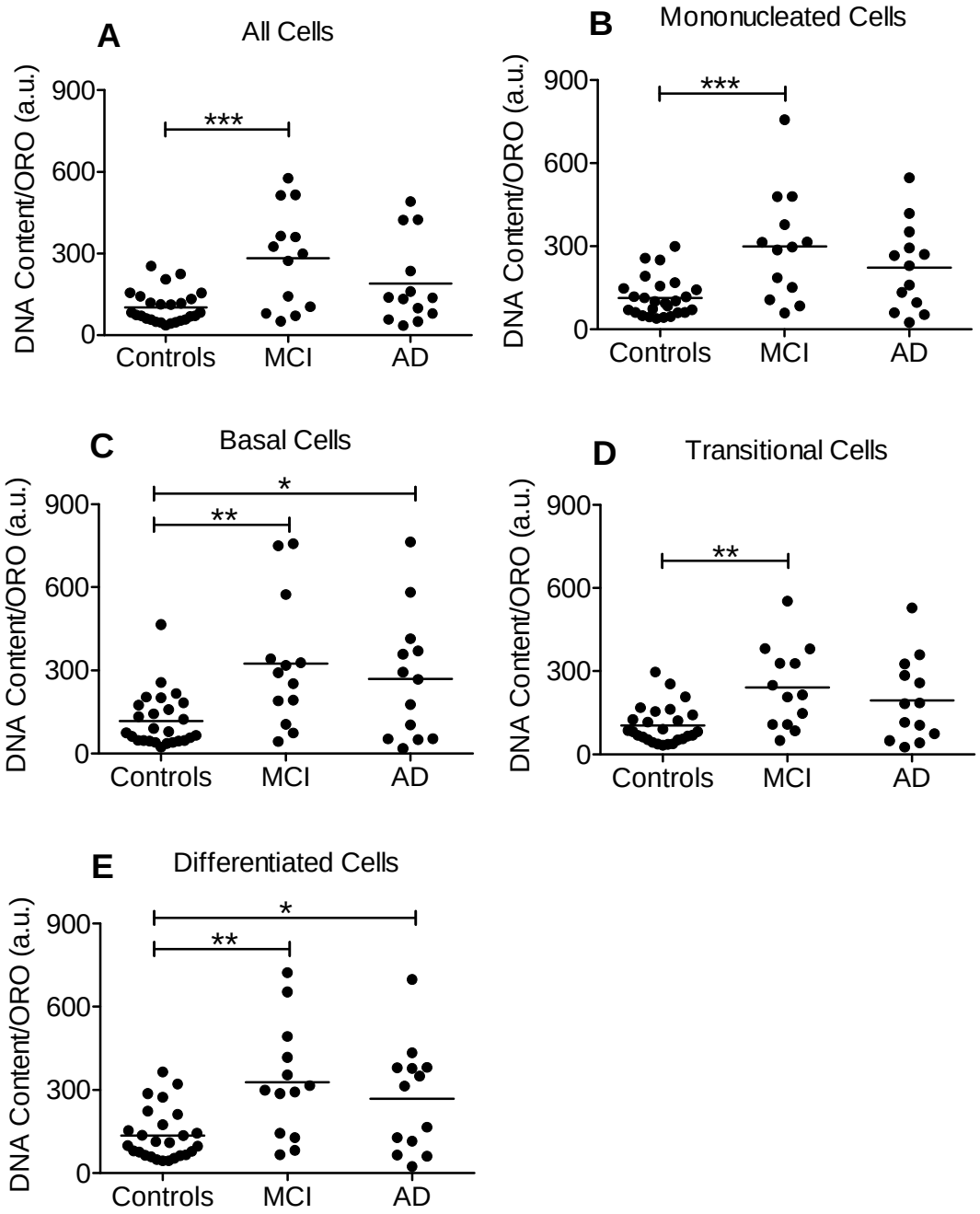
A
All Cells
DNA Content/ORO (a.u.)
900
600
300
0
***
Controls
MCI
AD
B
Mononucleated Cells
DNA Content/ORO (a.u.)
900
600
300
0
***
Controls
MCI
AD
C
Basal Cells
DNA Content/ORO (a.u.)
900
600
300
0
*
**
Controls
MCI
AD
D
Transitional Cells
DNA Content/ORO (a.u.)
900
600
300
0
**
Controls
MCI
AD
E
Differentiated Cells
DNA Content/ORO (a.u.)
900
600
300
0
*
**
Controls
MCI
AD

Figure 5.

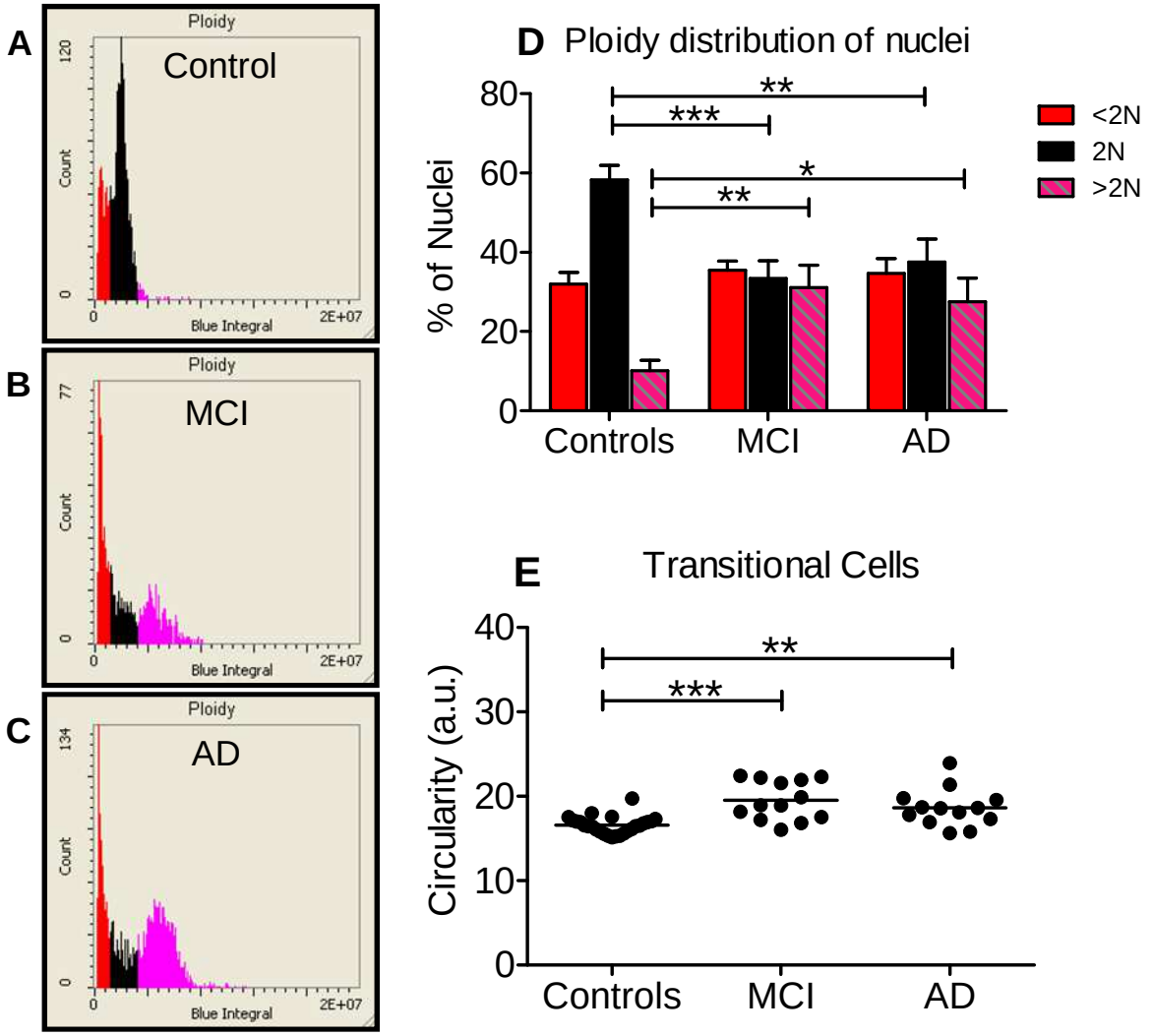
A
Ploidy
Control
Count
Blue Integral
B
Ploidy
MCI
Count
Blue Integral
C
Ploidy
AD
Count
Blue Integral
D Ploidy distribution of nuclei
% of Nuclei
<2N
2N
>2N
Controls
MCI
AD
E
Transitional Cells
Circularity (a.u.)
Controls
MCI
AD